

# Journal of Biomedical Optics

[SPIEDigitalLibrary.org/jbo](http://SPIEDigitalLibrary.org/jbo)

## **Ethidium bromide as a marker of mtDNA replication in living cells**

Anna Maria Villa  
Paola Fusi  
Valentina Pastori  
Giulia Amicarelli  
Chiara Pozzi  
Daniel Adlerstein  
Silvia Maria Doglia



**SPIE**

# Ethidium bromide as a marker of mtDNA replication in living cells

Anna Maria Villa,<sup>a</sup> Paola Fusi,<sup>a</sup> Valentina Pastori,<sup>a</sup> Giulia Amicarelli,<sup>a</sup> Chiara Pozzi,<sup>a</sup> Daniel Adlerstein,<sup>b</sup> and Silvia Maria Doglia<sup>a</sup>

<sup>a</sup>University of Milano-Bicocca, Department of Biotechnology e Biosciences, P.za della Scienza 2, 20126 Milan, Italy

<sup>b</sup>DiaSorin SpA, Via Crescentino, 13040 Saluggia (VC), Italy

**Abstract.** Mitochondrial DNA (mtDNA) in tumor cells was found to play an important role in maintaining the malignant phenotype. Using laser scanning confocal fluorescence microscopy (LSCFM) in a recent work, we reported a variable fluorescence intensity of ethidium bromide (EB) in mitochondria nucleoids of living carcinoma cells. Since when EB is bound to nucleic acids its fluorescence is intensified; a higher EB fluorescence intensity could reflect a higher DNA accessibility to EB, suggesting a higher mtDNA replication activity. To prove this hypothesis, in the present work we studied, by LSCFM, the EB fluorescence in mitochondria nucleoids of living neuroblastoma cells, a model system in which differentiation affects the level of mtDNA replication. A drastic decrease of fluorescence was observed after differentiation. To correlate EB fluorescence intensity to the mtDNA replication state, we evaluated the mtDNA nascent strands content by ligation-mediated real-time PCR, and we found a halved amount of replicating mtDNA molecules in differentiating cells. A similar result was obtained by BrdU incorporation. These results indicate that the low EB fluorescence of nucleoids in differentiated cells is correlated to a low content of replicating mtDNA, suggesting that EB may be used as a marker of mtDNA replication in living cells. © 2012 Society of Photo-Optical Instrumentation Engineers (SPIE). [DOI: 10.1117/1.JBO.17.4.046001]

Keywords: confocal fluorescence microscopy; ethidium bromide; mitochondria; mtDNA nucleoids; mtDNA replication; ligation-mediated PCR; BrdU; human neuroblastoma cells.

Paper 11515 received Sep. 16, 2011; revised manuscript received Feb. 15, 2012; accepted for publication Feb. 20, 2012; published online Apr. 6, 2012.

## 1 Introduction

In addition to their central role in energy production and physiology of the cell, mitochondria play an important role in tumorigenesis, as they are involved in the malignant transformation and in the maintenance of the tumor phenotype.<sup>1,2</sup> In his pioneering studies more than 50 years ago,<sup>3,4</sup> Warburg showed that a key event in carcinogenesis was an injury to the respiratory machinery leading to an increased glycolysis. After these works, several mitochondrial DNA (mtDNA) mutations and alterations involving mtDNA replication<sup>4</sup> and transcription were reported for different kinds of cancers. In particular, mitochondrial genes were found to be overexpressed in many tumor cell lines,<sup>5–7</sup> and mtDNA synthesis was observed to be altered in Rous sarcoma virus transformed cells.<sup>8</sup> In addition, a few of these alterations, as mtDNA depletion, seems to affect cancer progression.<sup>9</sup> All these findings indicate that mtDNA synthesis and transcription are crucial issues in tumor transformation. The study of mitochondrial DNA activity and organization in tumor cells is, therefore, central to understanding the role of mtDNA in the malignant transformation.

It is now well known that mtDNA is organized in nucleoprotein complexes called nucleoids.<sup>10</sup> Even if these complexes were not found to contain histone-like proteins, they contain DNA transaction factors and high-mobility group (HMG)-like proteins. Among these proteins, TFAM—which is a putative mtDNA packaging protein<sup>11</sup>—was found to play a fundamental role in mtDNA replication and transcription. Interestingly, it has

been recently shown by site-specific DNA methyltransferases<sup>12</sup> that the interaction of human mtDNA with TFAM can modulate its exposure to methylation depending on the mtDNA activity. In particular, the accessibility to mtDNA tranferase—a probe of mtDNA surface exposure—was found to be higher in nucleoids during replication but lower in the presence of oxidative stress damaging mtDNA. Additionally, as shown by M. Kucej et al.,<sup>13</sup> the structure of nucleoids in yeast was observed to change in response to the growth environment, a more open structure corresponding to respiring conditions. All these findings demonstrate that nucleoids dynamically respond to the cell needs and to the environment by changing their protein organization and mtDNA conformation and underline the need to study nucleoids in living cells in order to understand their dynamics. In living cells, nucleoids have been studied by noninvasive fluorescence microscopy, targeting fluorescent proteins to nucleoids,<sup>10,14</sup> or using supravital nucleic acid fluorescent probes, like ethidium bromide (EB)<sup>10,15–17</sup> and ditercalinium chloride (DC).<sup>18</sup>

We should recall that EB is an intercalating nucleic acid probe widely used to quantify the DNA content in fixed cells. On the contrary, it has been shown that in living cells nuclear DNA accessibility to EB is restricted only to a few DNA regions in active replication and/or transcription.<sup>19</sup> Moreover, it has been demonstrated that in living cells EB stains mtDNA in nucleoids with fluorescence intensity that varies from one nucleoid to the other.<sup>15,17</sup> A similar result was also obtained for DC,<sup>18</sup> which is also an intercalating nucleic acid fluorescent probe. It has been also reported that EB blocks mtDNA replication,<sup>20,21</sup> inhibits DNA polymerase  $\gamma$ ,<sup>22</sup> and

Address all correspondence to: Anna Maria Villa, University of Milano-Bicocca, Department of Biotechnology e Biosciences, P.za della Scienza 2, 20126 Milan, Italy; Tel: + 39 02 6448 3447; E-mail: annamaria.villa@unimib.it.

that a long-term exposition to EB is used to deplete human cells of their mtDNA.<sup>23</sup> In spite of this long-term toxicity, EB has been shown to stain mitochondria nucleoids in living cells without affecting cell viability and mitochondria morphology when measurements are performed on a time scale of about 1 h.<sup>10,15–17</sup>

All these data strongly suggest that EB in living cells interacts with actively replicating mtDNA and that EB fluorescence is enhanced upon this interaction. The differences in nucleoid fluorescence intensity may be therefore related to a different conformational status of mtDNA, depending on its replication or transcription.

In previous papers, we have studied the intracellular distribution and morphology of mitochondria in carcinoma cells and found that two mitochondria populations were present,<sup>24</sup> characterized by a very different EB fluorescence intensity.<sup>17</sup> These findings seem to suggest that in these cells the two mitochondria populations have a different mtDNA replication and/or transcription status, possibly related to cell motility and invasiveness. However, to prove in living cells the correlation between the intensity of EB fluorescence in nucleoids and the mtDNA activity, it has been necessary to work on a model system where the mtDNA replication state could be modulated and controlled. With this aim, in the present paper we investigated SHSY-5Y human neuroblastoma cells, which can differentiate into a neuronal phenotype when treated with retinoic acid (RA).<sup>25–27</sup> Indeed, mitochondria play a relevant role in the nervous system because of the neurons' high energy demand. It is through the regulation of their biogenesis that mitochondria allow neurons to meet their changing energy needs. However, opposite to what is found in tumor cells, which are characterized by an enhanced mtDNA synthesis,<sup>8</sup> neurons have a very low basal mtDNA replication activity,<sup>28</sup> making the SHSY-5Y neuroblastoma cell line a good model system to study the interaction of EB with mtDNA in different replicative conditions.

In the present work, the level of EB fluorescence in nucleoids of SHSY-5Y cells under living conditions has been evaluated by laser scanning confocal fluorescence microscopy (LSCFM) with photon counting detection. In order to correlate the fluorescence intensity of EB in mitochondria nucleoids with the replicative status of mtDNA, BrdU incorporation was also evaluated by confocal microscopy. In addition, ligation-mediated PCR (LMPCR) assay<sup>29,30</sup>—a technique that allows the quantification of nascent replicating mtDNA strands—was performed to estimate the level of mtDNA replication before and after SHSY-5Y cell differentiation induced by RA.

The results of all these approaches enabled us to correlate the EB fluorescence intensity with the mtDNA replication state in nucleoids of SHSY-5Y cells.

## 2 Materials and Methods

### 2.1 Chemicals

Rhodamine 123 and ethidium bromide were purchased from Molecular Probes (Eugene, OR). The concentration of the stock solutions of R123 and EB in water (10  $\mu$ M) were determined spectrophotometrically.

### 2.2 Cell Cultures

SHSY-5Y neuroblastoma cells were plated on twelve 100-mm plates (1  $\times$  10<sup>6</sup> cells/plate) in DMEM F12 (Lonza Group Ltd.,

Basel, Switzerland); after 24 h, the medium of six plates was replaced with fresh medium containing 10- $\mu$ M retinoic acid. Normal DMEM F12 was added to the other six plates, and all the cells were left to grow for 72 h and then harvested.

### 2.3 Confocal Fluorescence Microscopy

The EB fluorescence of mitochondria in living SHSY-5Y cells was studied using the Bio-Rad MRC-600 laser scanning confocal microscope (Bio-Rad, Hemel Hempstead, UK) equipped with an upright epifluorescence microscope Nikon Optiphot-2 (Nikon, Tokyo, Japan), carrying an oil immersion 60 $\times$  Nikon Planapochromat objective (N.A. = 1.4). EB fluorescence was excited by the 488-nm line of Argon ion laser, and fluorescence emission was collected through a long-pass filter above 515 nm. Photon counting detection was employed to keep the laser excitation power below 0.1 mW at the entry of the optical head. This condition minimized cell damages, a crucial requirement for the study of mitochondria in living cells.

In the photon counting collection mode, the black level of the photomultiplier is set to a reproducible value, and the frames are summed up by using the accumulation mode. Linearity was accomplished by automatically stopping the accumulation when one pixel reached the maximum limit value of 255. This allows us to compare the fluorescence intensity of different images using a simple normalization for the total number of accumulated frames.

For the confocal microscopy observations, cells were seeded in 35-mm Petri dishes and grown to reach 50% of confluence. Then cells were washed twice with phosphate buffer saline (PBS) (Sigma, St. Louis, MO, USA) and incubated in the medium at 37°C, 5% CO<sub>2</sub> in the presence of the appropriate dye. After incubation, cells were washed twice with PBS, and a coverslip was placed over the cells. Cells were incubated with 1- $\mu$ M R123 for 10 min, or with 1- $\mu$ M EB for 30 min. In the double-staining experiment, cells were incubated with 1  $\mu$ M EB for 30 min, and a small volume of an R123 stock solution was added after 20 min to reach the final concentration of 1  $\mu$ M.

For the immunofluorescence analysis, SHSY-5Y cells were plated onto coverslips (2  $\times$  10<sup>4</sup> cells/coverslip) coated with poly-lysine (Sigma St. Louis, MO, USA); after 24 h the medium was replaced with fresh medium containing 10- $\mu$ M retinoic acid (Sigma, St. Louis, MO, USA) or with normal DMEM F12. After 72 h cells were fixed for 10 min in cold MetOH at –20°C. Permeabilization was carried out by incubating the cells in the presence of 0.3% (w/v) saponin in PBS (7 min for three times). Cells were then stained with anti-COXIV (cytochrome oxidase IV) rabbit polyclonal antibody (1:250) (Abcam, Cambridge, UK). After extensive washes, cells were incubated with donkey anti-rabbit Cy2 conjugated antibody (1:150) (Jackson ImmunoResearch laboratories, West Grove, PA, USA). Incubations and washes were carried out at room temperature in PBS, 0.3% (w/v) saponin.

For BrdU analysis SHSY-5Y cells were plated onto coverslips (2  $\times$  10<sup>4</sup> cells/coverslip) coated with poly-lysine (Sigma St. Louis, MO, USA); after 24 h the medium of coverslips was replaced with fresh medium containing 10- $\mu$ M retinoic acid or with normal DMEM F12. After 72 h, cells treated with 10- $\mu$ M BrdU (Sigma St. Louis, MO, USA) for 1 h or 24 h were fixed for 20 min in 3% (w/v) paraformaldehyde in PBS and then incubated for 30 min in 2 M HCl at 37°C. Cells were blocked for 30 min in PBS, 1% (v/v) Triton X-100 (Sigma St. Louis, MO, USA), 1% BSA (Sigma St.

Louis, MO, USA). Cells were then stained for 1 h with anti-BrdU mouse monoclonal antibody (1:50) (Santa Cruz Biotechnology Inc. Santa Cruz, CA USA). After extensive washes in PBS, cells were incubated for 1 h with donkey anti-mouse Alexa Fluor 488 conjugate (1:200) (Invitrogen UK Ltd. Paisley, England) in PBS, 1% Triton X-100, 1% BSA.

Image analysis was performed on LSCFM 8-bit images with 256 gray levels. The mean EB fluorescence intensity was evaluated by using the LaserPix software (Bio-Rad, Hemel Hempstead, U.K.). The analysis was performed on more than 250 cells from 26 images. In the fluorescence images of the cells treated with EB, we traced areas of interest (AOI) limited to mitochondria nucleoids in order to collect only the signal coming from mtDNA, avoiding the contribution of the background due to EB bound to RNA. Since BrdU was incorporated also in nuclear DNA, the fluorescence images of BrdU treated cells were analyzed by using AOI centered only on the cell mitochondria to exclude the nuclear fluorescence. The maximum fluorescence intensity in each AOI was measured, and the mean fluorescence intensity for each experiment was calculated. About 200 cells for BrdU experiments were examined.

#### 2.4 Mitochondria Extraction

Mitochondria Isolation Kit for Cultured Cells (Pierce Biotechnology, Rockford, IL, USA) was used according to the manufacturer's instructions. Briefly, Reagent A was added to  $2 \times 10^7$  SHSY-5Y harvested cells, both differentiated and undifferentiated. After incubating 2 min on ice, Reagent B was added and incubation was carried out for 5 min on ice, vortexing every minute. Cells were subsequently resuspended in Reagent C and centrifuged at  $700 \times g$  for 10 min at 4°C. The supernatant was centrifuged at  $3000 \times g$  for 5 min at 4°C: the supernatant represented the cytosolic fraction, while the pellet contained the isolated mitochondria. Mitochondria were washed with Reagent C and centrifuged at  $12,000 \times g$  for 5 min at 4°C.

#### 2.5 Mitochondrial DNA Purification

Mitochondrial DNA was purified from isolated mitochondria using QIAamp DNA Micro kit from Qiagen (Qiagen, Hilden, Germany) following the protocol for isolation of genomic DNA from small volumes of blood reported in the manufacturer's instruction. Briefly, mitochondria from tumor and differentiated cells obtained from the previous step were resuspended in 100- $\mu$ l buffer ATL; 10- $\mu$ l Proteinase K (Invitrogen, Carlsbad, CA, USA) was added, followed by 100- $\mu$ l buffer A, vortexing for 15 sec. The mixture was then incubated for 10 min at 56°C; after 50- $\mu$ l ethanol addition, it was incubated for 3 min at room temperature. The lysate was then loaded onto MinElute Column (Qiagen, Germantown, MD, USA), which was washed with Buffer AW1 and Buffer AW2 by centrifugation. Elution was obtained adding 20- $\mu$ l distilled water and centrifuging, after a 1 min incubation at room temperature.

#### 2.6 Ligation-Mediated Real-Time PCR

We performed the ligation-mediated PCR (LMPCR) assay<sup>29,30</sup> to detect the newly synthesized H-strands with free 5' ends from two populations of mtDNA extracted from tumor SHSY-5Y cells before and after differentiation with retinoic acid. The first step of the protocol consists in extension of the primer GA137 (5' GAAGCAGATTGGGTACCAC 3') in

40- $\mu$ l reaction mixture containing 1x Thermo Pol reaction buffer (New England Biolabs, Ipswich, MA, USA), 200- $\mu$ M dNTPs mix (Fermentas, Ontario, Canada), 0.5 U Deep Vent exo<sup>-</sup> polymerase (New England Biolabs, Ipswich, MA, USA), 200-nM primer and 400-ng mtDNA extracted from SH5Y5 cells before and after treatment with retinoic acid, respectively. The mtDNA was denatured at 95°C for 5 min; the primer was annealed at 56°C for 30 min and extended at 75°C for 15 min.

The linker probe was produced using 40- $\mu$ M GA138 (5' GCGGTGACCCGGGAGATCTGTATTC 3') and 40  $\mu$ M GA139bis (5' OH GAATTCAGATC OH 3'). The two oligonucleotides were heated for 5 min at 95°C, shifted to 70°C and gradually cooled at room temperature to achieve a complete annealing into a dimer. After 1 h at room temperature, the solution was incubated at 4°C for 12 h and then stored in aliquots at -20°C.

Four  $\mu$ M of unidirectional linker was ligated to 30  $\mu$ l of target mtDNA on which the GA137 primer was previously extended. The 75- $\mu$ l reaction volume containing 200U T4 ligase and 1  $\times$  T4 ligase buffer (both from New England Biolabs, Ipswich, MA, USA) was incubated at 16°C overnight. Treated mtDNA was purified using QIAprep Spin Miniprep Kit (Qiagen, Hilden, Germany).

Six  $\mu$ l of the mtDNA treated as described above was amplified in the presence of 400 nM of both forward and reverse primer (GA140 5' GTGACCCGGGAGATCTGTATTC 3'; GA141 5' GCACATTACAGTCAAATCCCTTCTCGT 3') and 1  $\times$  iQ SYBR Green Supermix with Rox (Biorad, Hercules, CA, USA) in a total volume of 25  $\mu$ l, and monitored on the ABI 7500 Real Time PCR instrument (Applied Biosystems, Fostercity, CA, USA). The thermal protocol consisted of an initial denaturation at 95°C for 2 min, followed by 45 cycles of 95°C for 10 sec and 60°C for 45 sec. The Ct values of fluorescence were obtained for each sample analyzed, and the Ct average was calculated after 13 repetitions.

The extension-ligation protocol was conducted for six independent times in triplicate on mtDNA from two different SHSY-5Y cultures, both consisting of tumoral and retinoic acid differentiated cells.

### 3 Results

#### 3.1 Laser Scanning Confocal Microscopy of Ethidium Bromide Fluorescence

The transmission image and the confocal fluorescence image of the intracellular distribution of EB in human neuroblastoma SHSY-5Y cells are reported in Figs. 1(a) and 1(b), respectively. As can be seen in Fig. 1(a), these cells grow as a monolayer and form large clusters of adherent cells with epithelioid morphology. In the confocal fluorescence image [Fig. 1(b)], highly fluorescent spots of EB can be observed in mitochondria, superimposed to the diffuse EB fluorescent background of the mitochondria matrix. In the higher magnification images reported in Figs. 1(c) and 1(d), it is possible to identify these spots as mitochondria nucleoids, as reported for 143B osteosarcoma cells after EB staining.<sup>10</sup> The EB diffuse fluorescence along each organelle, instead, is likely due to the staining of the RNA present in the mitochondria matrix.

To better visualize the mitochondria in the examined cells, we also performed a double staining experiment using—in addition to EB—Rhodamine 123 (R123), which is a

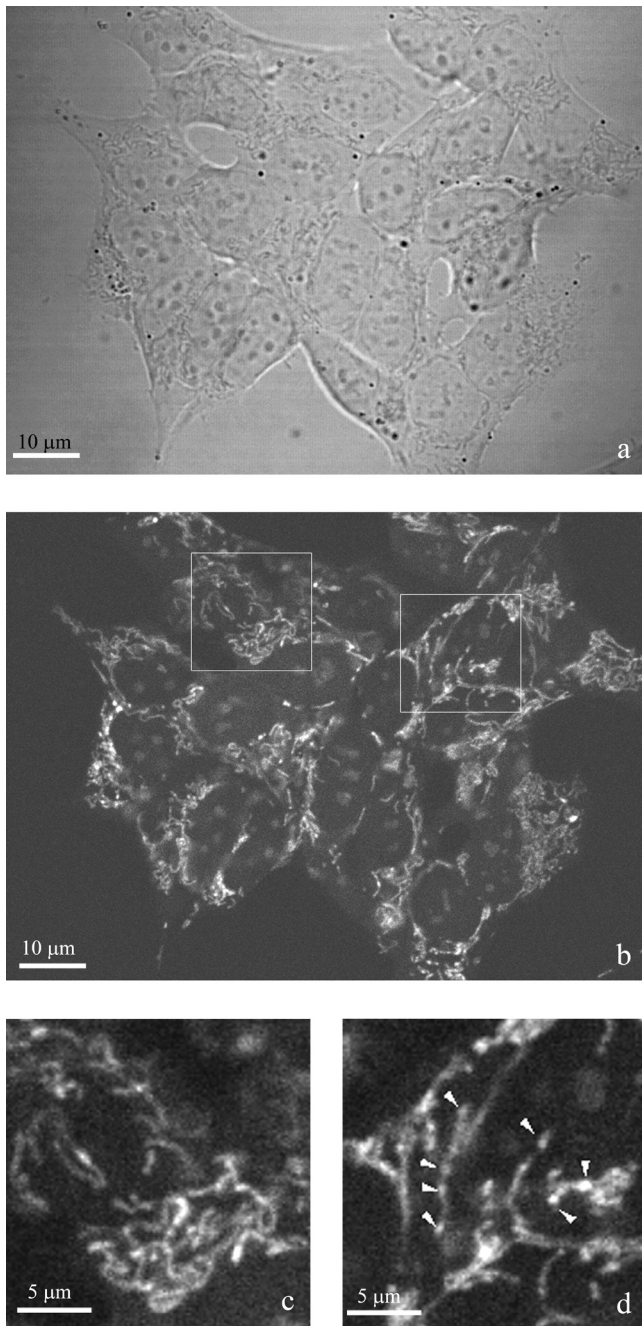


**Fig. 1** Laser scanning confocal fluorescence microscopy (LSCFM) of SHSY-5Y cells treated with  $1\text{-}\mu\text{M}$  EB for 30 min: (a) transmission image; (b) fluorescence image; (c) and (d) enlarged images of mitochondria in (b); mitochondria nucleoids can be seen as fluorescent spots (arrowheads) along the organelles.

well-known potentiometric probe of mitochondria in living cells. The EB fluorescent image and the R123 image are reported, respectively, in Figs. 2(a) and 2(c). Both probes are localized in mitochondria, but their fluorescence distribution pattern is different. While R123 probes the mitochondrial potential [Figs. 2(c) and 2(d)], EB staining shows highly fluorescent nucleoids inside each mitochondrion [Figs. 2(a) and 2(b)]. When SHSY-5Y cells were induced to differentiate by treatment with retinoic acid (RA) ( $10\text{ }\mu\text{M}$  for 72 h), they underwent a morphological change into a neuronal phenotype, protruding their neurites into the extracellular space.<sup>26</sup> In Fig. 3, using cytochrome

oxidase IV (COX) immunofluorescence, we compared the SHSY-5Y cells before and after differentiation. As can be seen, before differentiation the cells displayed an epithelioid morphology [Fig. 3(a)], while after differentiation [Fig. 3(b)] they acquired an elongated morphology with the formation of long neurites, responsible for a reduced adherence to the substrate. Moreover, differentiated cells were characterized by a smaller cytoplasm and by a reduced number of mitochondria [Fig. 3(b)] compared to the undifferentiated SHSY-5Y tumor cells [Fig. 3(a)]. Similar images were obtained by EB staining, both for tumor [Figs. 4(a) and 4(b)] and differentiated cells [Figs. 4(c), 4(d), and 5]. Interestingly, in the differentiated cells the overall EB fluorescence was found to be appreciably reduced after 72 h of RA treatment [Fig. 4(c)], even though at this stage only a fraction of the cell population assumed a neuronal morphology. This result indicated that all the differentiating cells displayed a reduction of their EB fluorescence intensity, independently of the phase reached by each cell in its morphological transformation [Figs. 4(c) and 5]. In particular, the EB fluorescent nucleoids in these differentiating cells were found to be strongly reduced in number, compared with undifferentiated tumour cells. The EB fluorescence background along each organelle was also reduced, a result that indicates a decrease in the content of mitochondrial RNA in the differentiated cells.

Interestingly, a lower R123 fluorescence was also observed in differentiating cells, a result that could reflect a reduced mitochondria membrane potential following RA treatment (data not shown).

### 3.2 Laser Scanning Confocal Microscopy of BrdU

To monitor the level of mtDNA synthesis in the examined cells, we used BrdU incorporation. In Fig. 6 the fluorescence and transmission confocal images of SHSY-5Y cells treated with BrdU and with an anti-BrdU antibody are reported before [Figs. 6(a) and 6(b)] and after [Figs. 6(c) and 6(d)] differentiation. As can be seen, BrdU is incorporated in the nuclei only of replicating cells [Fig. 6(a)], while fully differentiated cells, which do not replicate, show no nuclear fluorescence [Fig. 6(c)]. In contrast, it is difficult to appreciate a difference in BrdU mitochondria fluorescence between undifferentiated and differentiated cells only by comparing Figs. 6(a) and 6(c). Therefore, as reported in the next paragraph, an image analysis was performed to evaluate BrdU fluorescence in mitochondria nucleoids before and after differentiation.

### 3.3 Image Analysis

To evaluate the EB fluorescence intensity in of SHSY-5Y, an image analysis was performed on the LSCFM images using the LaserPix software (Bio-Rad, Hemel Hempstead, U.K.). In this analysis we have traced an AOI only comprising the regions inside mitochondria that contain nucleoids, therefore reducing the contribution of the fluorescence background due to EB bound to RNA. About 250 cells in 26 images were analyzed, after normalization of the image fluorescence signal to 100 accumulated frames. A mean EB fluorescence intensity of 120.1 (S.D. = 59.0) a.u. and of 40.6 (S.D. = 10.0) a.u. was obtained respectively for mitochondria before and after differentiation. Therefore, the EB fluorescence intensity ratio of mitochondria in tumor versus differentiated cells was found to be about 2.99 (Fig. 7).

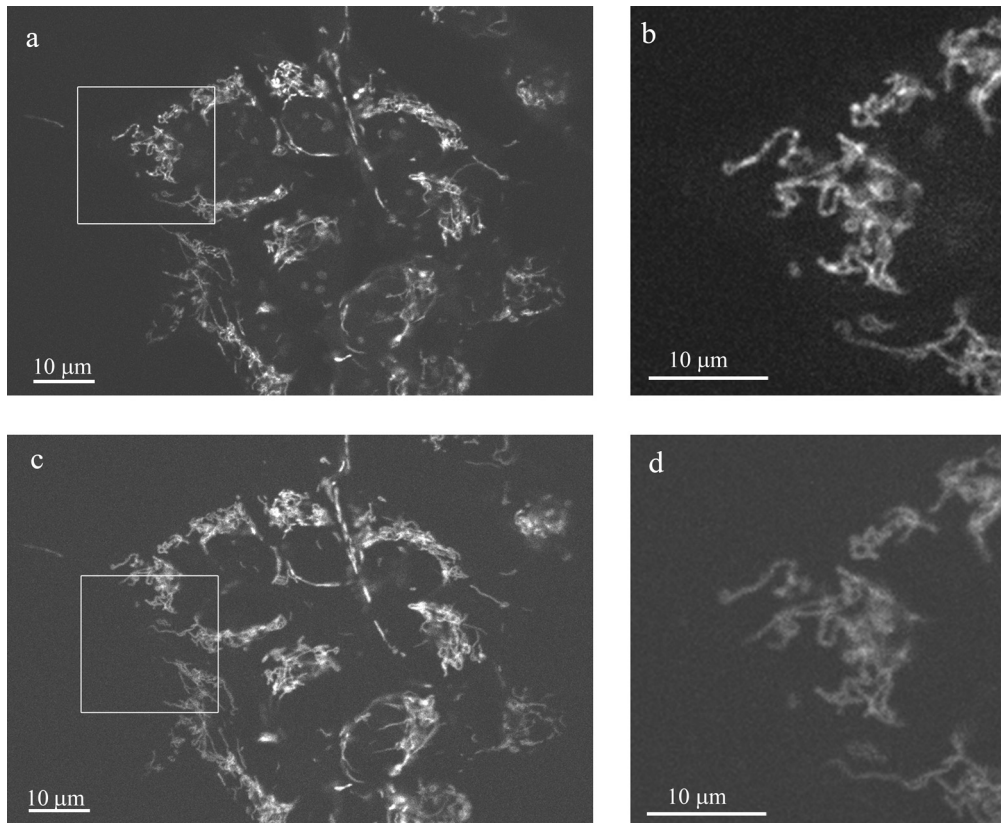


**Fig. 2** EB and R123 double-staining experiment. LSCFM images of SHSY-5Y cells. (a) and (b): EB fluorescence; (c) and (d): R123 fluorescence.

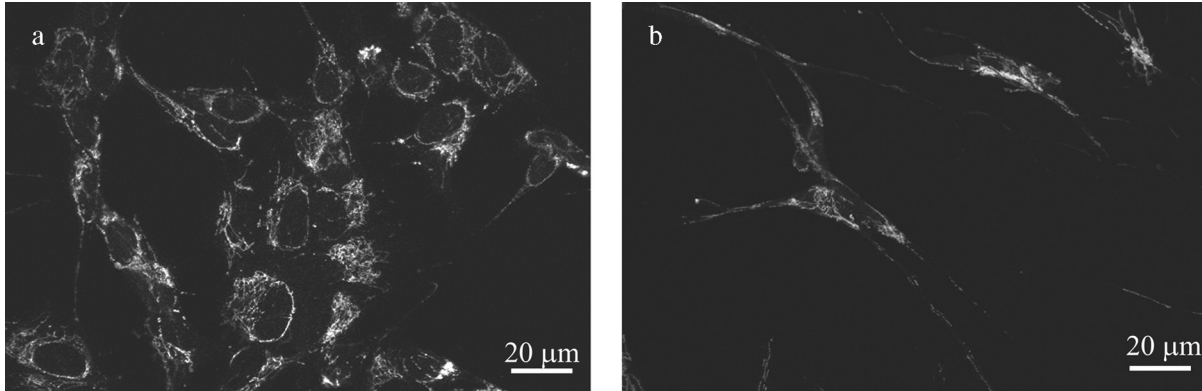


**Fig. 3** Immunofluorescence of COX (cytochrome oxidase IV) in mitochondria of SHSY-5Y cells: (a) before differentiation and (b) after differentiation with RA.

To determine the mtDNA newly synthesized by the SHSY-5Y cells, the BrdU labeling was performed, and the fluorescence intensity of the anti-BrdU antibody was measured by confocal fluorescence microscopy. Since BrdU is incorporated not only in mtDNA but also in nuclear DNA, the fluorescence images of the anti-BrdU antibody in mitochondria were analyzed by tracing an AOI around the regions of the images containing the cell mitochondria in order to exclude the nuclear fluorescence. When the cells were exposed to BrdU for 1 h, the mean fluorescence was 1267.5 (S.D. = 147.7) a.u. and 636.6 (S.D. = 99.1) a.u. before and after differentiation, respectively, after normalization of the images to 100 accumulated frames. Therefore, the BrdU fluorescence ratio of the SHSY-5Y tumor cells and that of the differentiated cells was found to

be about 1.99 after 1 h of BrdU incorporation. This ratio remained around two also after 24 h of BrdU incorporation (Fig. 8).

#### 3.4 *D-Loop Quantification in SHSY-5Y Cells Before and After Differentiation*

Polymerase Chain Reaction (PCR) is a technique to amplify a single or a few copies of DNA, generating millions of copies of a particular DNA sequence. The real-time PCR (RT-PCR) system<sup>31,32</sup> is based on the detection and quantitation of a fluorescent reporter, whose signal increases in direct proportion to the amount of DNA produced. The progress of the reaction is monitored in real time using a fluorescent marker whose fluorescence is

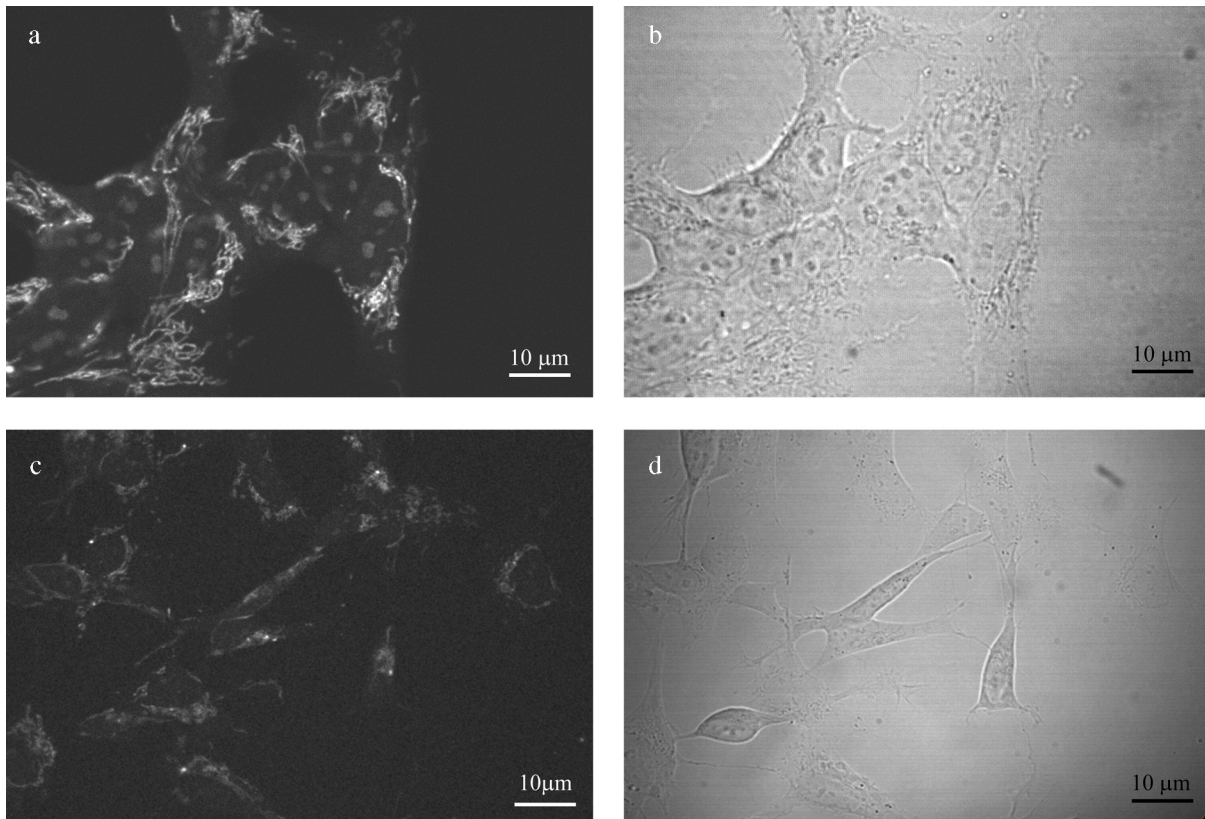


**Fig. 4** LSCFM images of SHSY-5Y cells: (a) EB fluorescence image before differentiation and (b) transmission image of the same field; (c) EB fluorescence image after differentiation with RA and (d) transmission image of the same field.

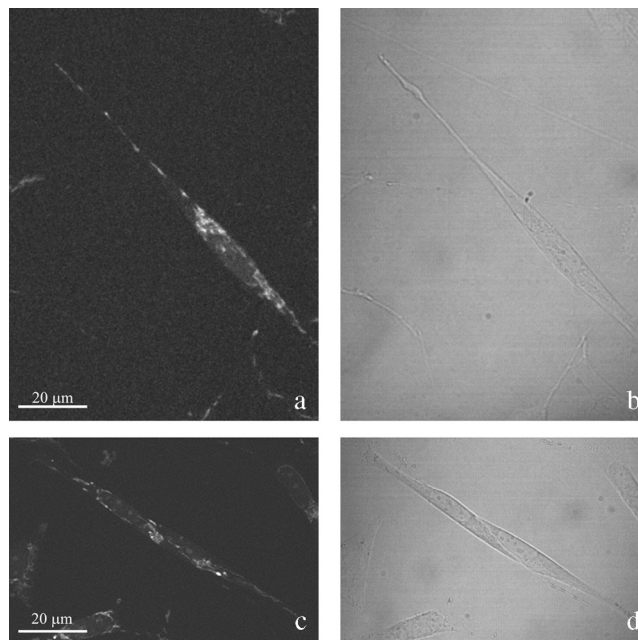


**Fig. 5** LSCFM images of SHSY-5Y cells after differentiation with retinoic acid. Cells were treated with 1- $\mu$ M EB for 30 min: (a) and (c) fluorescence; (b) and (d) transmission images. The measured fluorescence intensities were digitally enhanced of a factor three for a better visualization.

enhanced upon binding to DNA. The output can be graphically represented as a curve of increasing fluorescence against PCR cycles (amplification plot). A threshold of fluorescence intensity is set at a level where the amount of fluorescence is significantly higher than the background (usually 10 times the standard

deviation of the baseline). The point at which the amplification plot crosses the threshold is called cross threshold (Ct). This value is conventionally used to compare different samples. The higher the starting copy number of the nucleic acid target, the sooner the fluorescence threshold is reached.

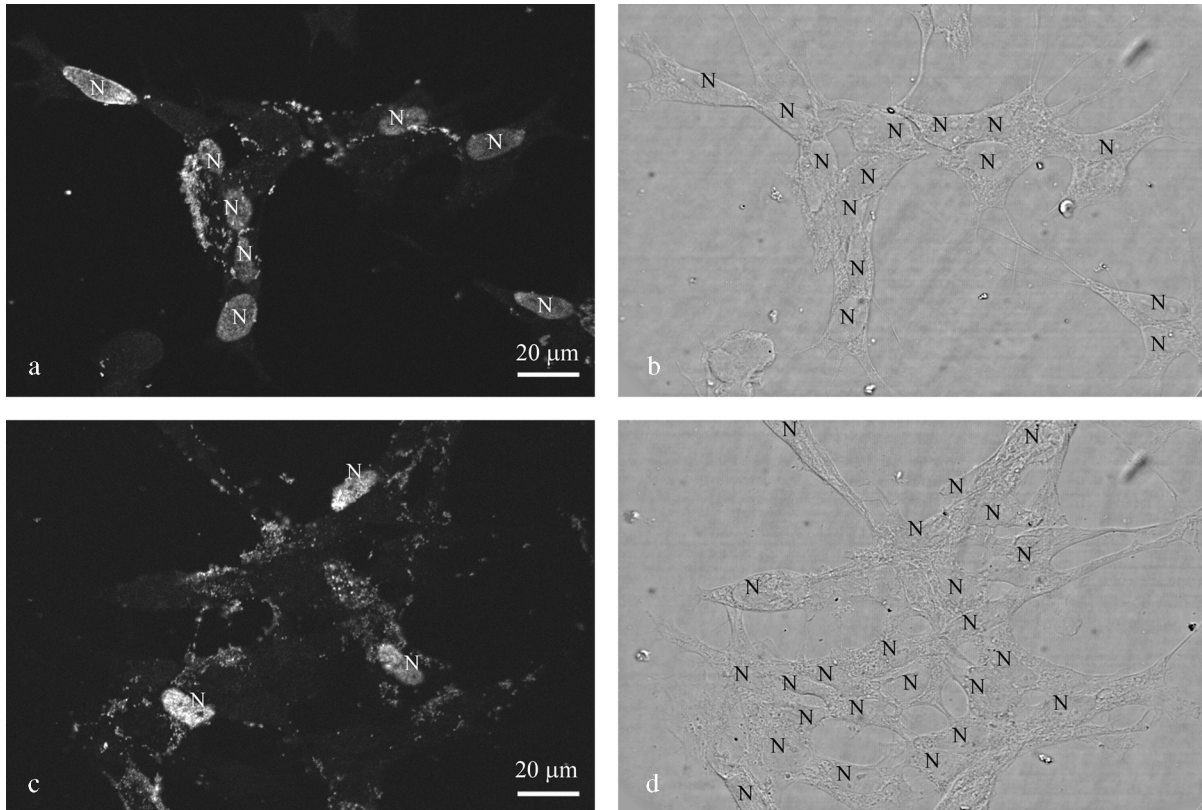


**Fig. 6** LSCFM of SHSY-5Y cells treated with 10- $\mu$ M BrdU for 1 h: (a) anti-BrdU antibody fluorescence image before differentiation and (b) transmission image of the same field; (c) anti-BrdU antibody fluorescence image after differentiation with RA and (d) transmission image of the same field. "N" indicates cell nuclei. Scale bar = 20  $\mu$ m.

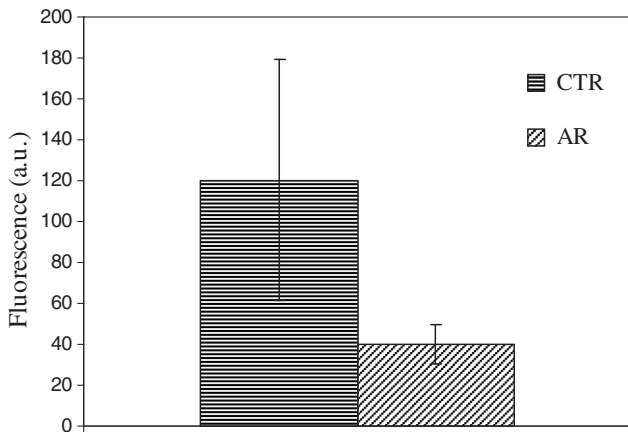


**Fig. 7** Mean fluorescence values calculated from the confocal images of the EB fluorescence in SHSY-5Y cells before (CTR) and after (AR) 72 h of differentiation. The reported values are obtained after normalization of the images to 100 accumulated frames.

In order to establish whether the EB fluorescence intensity reduction in differentiating cells was related to a reduced synthesis of mtDNA, the amount of nascent mtDNA strands in human neuroblastoma SHSY-5Y cells before and after differentiation with RA was evaluated by ligation-mediated PCR on a real-time instrument.

Mitochondrial DNA replication is coupled to transcription and is initiated from the single promoter on the light strand.<sup>33</sup> The resulting transcript forms a stable RNA:DNA hybrid, which

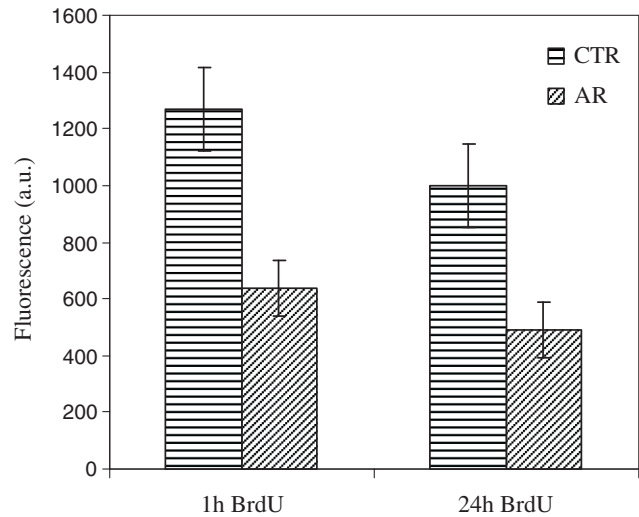


**Fig. 8** Mean fluorescence values calculated from the confocal images of anti-BrdU antibody in SHSY-5Y cells before (CTR) and after (AR) 72 h of differentiation. The reported values are obtained after normalization of the images to 100 accumulated frames. Data for BrdU incorporation times of 1 h and 24 h are shown.

is processed by the enzyme RNase MRP. This enzyme cleaves the RNA into fragments, which are then used as replication primers for the mtDNA polymerase  $\gamma$  (pol  $\gamma$ ). Most of these replication strands are prematurely terminated after being extended by several hundred nucleotides. These terminated strands are known collectively as 7S DNA. A unique structure named

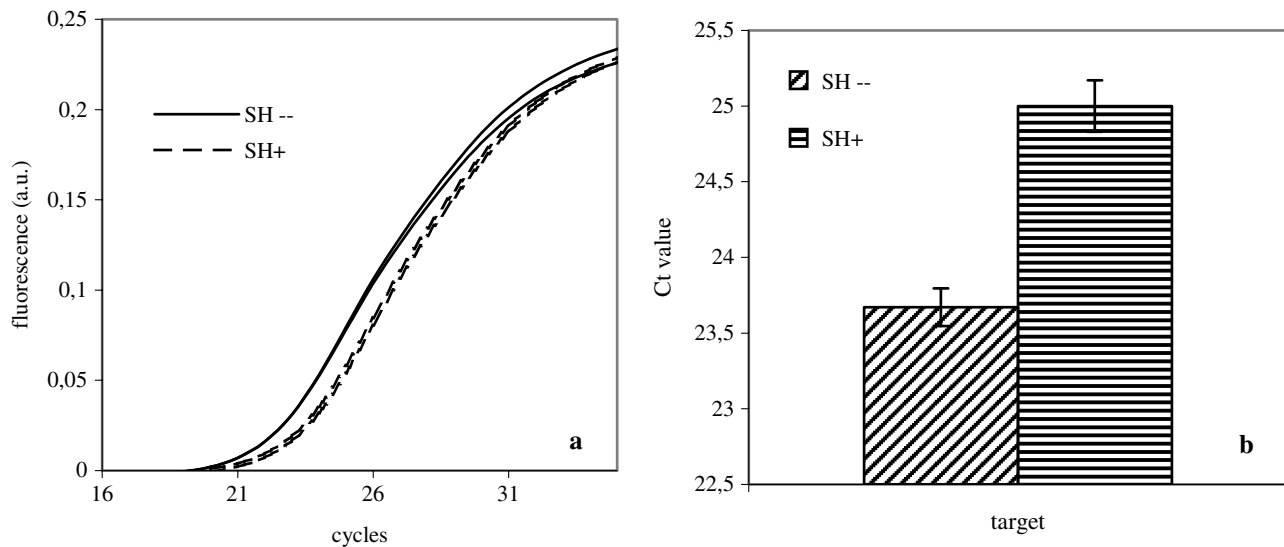


**Fig. 9** Ligation Mediated PCR of SHSY-5Y cell mtDNA: (a) example of ligation-mediated real time PCR on mtDNA extracted from SHSY-5Y cells, before (SH-) and after (SH+) differentiation with RA; (b) threshold cycle value obtained by ligation-mediated real time PCR on mtDNA from SHSY-5Y cells, before (SH-) and after (SH+) differentiation.

the displacement loop (D-loop) is formed when a 7S DNA remains bound to the parental molecule and displaces one of the duplex parental strands. It has been estimated that 95% of all the synthesized leading replication strands are prematurely terminated in this manner.<sup>34</sup> Therefore, much of the DNA synthesis within mitochondria is devoted to regenerating 7S DNA, with consequent formation of the D-loop.

The quantitative measurement of the D-loops was achieved detecting the intercalating dye SYBR green, whose level of fluorescence is proportional to the obtained PCR product. The time needed to reach the established threshold fluorescence is proportional to the initial amount of DNA. As described in Material and Methods, mtDNA from both differentiated and not differentiated cells was treated and amplified in parallel. The reactions were monitored in real time, and the respective threshold cycles were calculated and compared.

The results of this approach demonstrated that the DNA from undifferentiated cells is amplified before that of differentiated ones, indicating a higher amount of starting material. In particular, we found that mtDNA samples from differentiated SHSY-5Y cells were amplified with a threshold cycle value of  $25 \pm 0.25$ , while the main Ct of undifferentiated SHSY-5Y cells was  $23.67 \pm 0.34$  [Fig. 9(a)]. Comparing the Ct obtained, we observed  $1.33 \pm 0.42$  cycles of difference between the undifferentiated and differentiated samples [Fig. 9(b)], indicating that undifferentiated cells contain 2.51 times ( $2^{1.33}$ ) more replicating D-loops than differentiating ones. This result is in agreement with the value of 2.99 obtained from the EB fluorescence intensity analysis performed on the LSCFM images.

#### 4 Discussion

In this work we studied the correlation between the fluorescence intensity of EB in mitochondria nucleoids of living cells and the replication activity of mtDNA. We modulated the mtDNA replication state of human neuroblastoma SHSY-5Y cells by inducing differentiation with retinoic acid, and we compared the EB fluorescence intensity, as detected by LSCFM, before and after differentiation.

We found that when SHSY-5Y cells were treated with EB before differentiation, highly fluorescent nucleoids were observed in mitochondria. Moreover, the fluorescence intensity of EB in nucleoids was observed to vary even within the same organelle, indicating that the interaction of EB with mtDNA is rather heterogeneous. When SHSY-5Y cells were induced to differentiate by RA, a lower number of nucleoids were observed, characterized also by a reduced fluorescence. Through image analysis, the mean EB mitochondria fluorescence intensity was found to be  $62.9$  (S.D. =  $24.6$ ) a.u. and  $40.6$  (S.D. =  $10.0$ ) a.u., respectively, in undifferentiated and in differentiated cells, corresponding to a ratio between undifferentiated and differentiated cells of about 1.55.

It is well known that, when mtDNA is replicating, a D-loop structure is formed, which is characterized by a DNA triple helix. This triple helix has been proved to bind EB in solution and to induce an appreciable fluorescence enhancement, as found for EB intercalation in the DNA double helix.<sup>35,36</sup> In this perspective, the higher EB fluorescence intensity in undifferentiated tumor cells suggests a higher accessibility of mtDNA to EB in these cells compared with that in the differentiated neuronal cells, where a reduced mtDNA replication activity is expected.

To demonstrate the correlation between the fluorescence intensity of EB in nucleoids and the replicative status of the mtDNA, we investigated SHSY-5Y cells, before and after differentiation, using immunocytochemistry analysis and ligation mediated PCR.

After labeling the newly synthesized DNA with BrdU, the fluorescent anti-BrdU antibody was observed in several nuclei and in a punctate pattern within the cytoplasm of both undifferentiated and differentiated SHSY-5Y cells. As reported in the literature,<sup>37</sup> this punctate fluorescence pattern corresponds to sites of mtDNA synthesis in mitochondria. By image analysis, we evaluated the mean BrdU fluorescence localized in SHSY-5Y nucleoids and found an intensity of  $1267.5$  (S.D. =  $147.7$ ) a.u. and  $636.6$  (S.D. =  $99.1$ ) a.u., respectively, before and after differentiation. After 1 h of BrdU incorporation, the ratio of

BrdU fluorescence tumor versus that in differentiated cells was about two, a value that remained stable even after 24 h.

In addition, we validate these results evaluating by LMPCR the amount of nascent mtDNA strands in SHSY cells before and after differentiation. We found that the number of replicating D-loops in tumor undifferentiated cells is about 2.5 folds that in differentiated cells, again confirming a higher replicative activity of mtDNA in SHSY-5Y cells before differentiation. This result demonstrates that the fluorescence intensity observed by LSCFM is correlated to the level of replicating mtDNA.

## 5 Conclusions

In this work we demonstrate that the intensity of EB fluorescence in the nucleoids of living SHSY-5Y cells is correlated with the replication status of their mtDNA. In particular, we found that mtDNA has a higher replication activity in tumor undifferentiated cells than in differentiated neuronal cells, suggesting that the accessibility of mtDNA to EB is higher during replication. These results, therefore, indicate that EB can be taken as a supravital marker of replicating mtDNA in living cells. Moreover, they confirm that the two mitochondria populations with different EB fluorescence that we observed in living carcinoma cells<sup>17</sup> are indeed characterized by a different mtDNA replication activity, probably due to a different role in mitochondria biogenesis of carcinoma cells.

The marked differences in mtDNA replication level reported here for tumor and differentiated cells suggest to investigate the possible use of EB as a marker of tumor transformation, allowing also to recognize the presence of specialized mitochondria subpopulations in the cell.

## Acknowledgments

We thank Carla Smeraldi for kindly revising the language. S.M.D. and P.F. acknowledge the financial support of the grant F.A.R. (Fondo di Ateneo per la Ricerca) of the University of Milano-Bicocca.

## References

- V. Gogvadze, S. Orrenius, and B. Zhivotovsky, "Mitochondria in cancer cells: what is so special about them," *Trends Cell Biol.* **18**(4), 165–173 (2008).
- G. Kroemer, "Mitochondria in cancer," *Oncogene* **25**(34), 4630–4632 (2006).
- O. Warburg, "On respiratory impairment in cancer cells," *Science* **124**(3215), 269–270 (1956).
- O. Warburg, "On the origin of cancer cells," *Science* **123**(3191), 309–314 (1956).
- N. Glaichenhaus, P. Leopold, and F. Cuzin, "Increased levels of mitochondrial gene expression in rat fibroblast cells immortalized or transformed by viral and cellular oncogenes," *EMBO J.* **5**(6), 1261–1265 (1986).
- I. Nikolaev et al., "Increased expression of several mitochondrial genes in human and monkey B-cell non-Hodgkin lymphomas," *Mol. Biol. Cell* **35**(1), 108–114 (2001).
- S. Grandemange et al., "Stimulation of mitochondrial activity by p43 overexpression induces human dermal fibroblast transformation," *Cancer Res.* **65**(10), 4282–4291 (2005).
- M. A. D'Agostino and M. M. Nass, "Specific changes in the synthesis of mitochondrial DNA in chick embryo fibroblasts transformed by Rous sarcoma viruses," *J. Cell Biol.* **71**(3), 781–794 (1976).
- M. Higuchi, "Regulation of mitochondrial DNA content and cancer," *Mitochondrion* **7**(1–2), 53–57 (2007).
- J. N. Spelbrink et al., "Human mitochondrial DNA deletions associated with mutations in the gene encoding Twinkle, a phage T7 gene 4-like protein localized in mitochondria," *Nat. Genet.* **28**(3), 223–231 (2001).
- T. I. Alam et al., "Human mitochondrial DNA is packaged with TFAM," *Nucleic Acids Res.* **31**(6), 1640–1645 (2003).
- A. P. Rebelo, S. L. Williams, and C. T. Moraes, "In vivo methylation of mtDNA reveals the dynamics of protein-mtDNA interactions," *Nucleic Acids Res.* **37**(20), 6701–6715 (2009).
- M. Kucej et al., "Mitochondrial nucleoids undergo remodeling in response to metabolic cues," *J. Cell Sci.* **121**(Pt 11), 1861–1868 (2008).
- N. Garrido et al., "Composition and dynamics of human mitochondrial nucleoids," *Mol. Biol. Cell* **14**(4), 1583–1596 (2003).
- F. J. Iborra, H. Kimura, and P. R. Cook, "The functional organization of mitochondrial genomes in human cells," *BMC Biol.* **2**(9), 1–14 (2004).
- K. Kasashima et al., "Human prohibitin 1 maintains the organization and stability of the mitochondrial nucleoids," *Exp. Cell Res.* **314**(5), 988–996 (2008).
- A. M. Villa and S. M. Doglia, "Ethidium bromide as a vital probe of mitochondrial DNA in carcinoma cells," *Eur. J. Cancer* **45**(14), 2588–2597 (2009).
- M. Okamoto et al., "Ditercalinium chloride, a pro-anticancer drug, intimately associates with mammalian mitochondrial DNA and inhibits its replication," *Curr. Genet.* **43**(5), 364–370 (2003).
- M. Tramier et al., "Restrained torsional dynamics of nuclear DNA in living proliferative mammalian cells," *Biophys. J.* **78**(5), 2614–2627 (2000).
- R. D. Leibowitz, "The effect of ethidium bromide on mitochondrial DNA synthesis and mitochondrial DNA structure in HeLa cells," *J. Cell Biol.* **51**(1), 116–122 (1971).
- T. Hayakawa et al., "Ethidium bromide-induced inhibition of mitochondrial gene transcription suppresses glucose-stimulated insulin release in the mouse pancreatic beta-cell line betaHC9," *J. Biol. Chem.* **273**(32), 20300–20307 (1998).
- L. Tarrago-Litvak et al., "The inhibition of mitochondrial DNA polymerase gamma from animal cells by intercalating drugs," *Nucleic Acids Res.* **5**(6), 2197–2210 (1978).
- M. P. King and G. Attardi, "Human cells lacking mtDNA: repopulation with exogenous mitochondria by complementation," *Science* **246**(4929), 500–503 (1989).
- A. M. Villa and S. M. Doglia, "Mitochondria in tumor cells studied by laser scanning confocal microscopy," *J. Biomed. Opt.* **9**(2), 385–394 (2004).
- S. Pahlman et al., "Differentiation and survival influences of growth factors in human neuroblastoma," *Eur. J. Cancer* **31A**(4), 453–458 (1995).
- L. Fontan-Gabas et al., "All-trans-retinoic acid inhibits collapsin response mediator protein-2 transcriptional activity during SH-SY5Y neuroblastoma cell differentiation," *FEBS J.* **274**(2), 498–511 (2007).
- G. Lopez-Carballo et al., "Activation of the phosphatidylinositol 3-kinase/Akt signaling pathway by retinoic acid is required for neural differentiation of SH-SY5Y human neuroblastoma cells," *J. Biol. Chem.* **277**(28), 25297–25304 (2002).
- G. J. Wang, L. M. Nutter, and S. A. Thayer, "Insensitivity of cultured rat cortical neurons to mitochondrial DNA synthesis inhibitors: evidence for a slow turnover of mitochondrial DNA," *Biochem. Pharmacol.* **54**(1), 181–187 (1997).
- T. A. Brown and D. A. Clayton, "Release of replication termination controls mitochondrial DNA copy number after depletion with 2',3'-dideoxycytidine," *Nucleic Acids Res.* **30**(9), 2004–2010 (2002).
- Y. Kai et al., "Mitochondrial DNA replication in human T lymphocytes is regulated primarily at the H-strand termination site," *Biochim. Biophys. Acta* **1446**(1–2), 126–134 (1999).
- R. Higuchi et al., "Kinetic PCR analysis: real-time monitoring of DNA amplification reactions," *Biotechnology (NY)* **11**(9), 1026–1030 (1993).
- J. Yguerabide and A. Ceballos, "Quantitative fluorescence method for continuous measurement of DNA hybridization kinetics using a fluorescent intercalator," *Anal. Biochem.* **228**(2), 208–220 (1995).
- G. S. Shadel and D. A. Clayton, "Mitochondrial DNA maintenance in vertebrates," *Annu. Rev. Biochem.* **66**, 409–435 (1997).
- D. Bogenhagen and D. A. Clayton, "Mechanism of mitochondrial DNA replication in mouse L-cells: kinetics of synthesis and turnover of the initiation sequence," *J. Mol. Biol.* **119**(1), 49–68 (1978).
- J. L. Mergny et al., "Intercalation of ethidium bromide into a triple-stranded oligonucleotide," *Nucleic Acids Res.* **19**(7), 1521–1526 (1991).
- P. V. Scaria and R. H. Shafer, "Binding of ethidium bromide to a DNA triple helix. Evidence for intercalation," *J. Biol. Chem.* **266**(9), 5417–5423 (1991).
- J. Magnusson et al., "Replication of mitochondrial DNA occurs throughout the mitochondria of cultured human cells," *Exp. Cell Res.* **289**(1), 133–142 (2003).